Railway multibody dynamics: modeling advances and industrial applications

José L. Escalona

Department of Mechanical and Manufacturing Engineering
University of Seville
Camino de los Descubrimientos s/n, 41092, Sevilla, Spain
escalona@us.es

ABSTRACT

This paper is a summary of the research done at the University of Seville in the field of railway dynamics in the last 20 years. This research is separated in this paper in two complementary lines: (1) the development of improved computational models for the dynamic analysis of rail vehicles and (2) on the development of experimental techniques for improved safety and maintenance of vehicles and tracks.

Keywords: Railway dynamics, railway multibody dynamics, track geometry measurement.

1 INTRODUCTION

Trains are safe, efficient, reliable, environmentally friendly… These ideas are repeated today in the media; however, the user experience may not exactly match that perception, which means that the train may not be always such an attractive transport option. There is there is a lot of room for improvement in rail transport technology. From the user's point of view, the train ride is sometimes annoying because it moves forward chaotically. When driving a car, you can keep the velocity approximately constant at the road even when many other cars surround your own at a relatively short distance. However, the train can be apparently alone in the track, but it stops from time to time, or it decreases drastically its speed without apparent reasons. On short or medium distance trains it is a common experience to be stopped in the countryside waiting for who knows what.

Density of trains in the track is far smaller that density of cars in the road. It is understandable that there should not be may aircrafts flying close to each other, but the same idea is not apparent for trains. Using autonomous vehicles would help to increase the trains density, and therefore to make the transport more efficient, without compromising safety. Massive use of autonomous cars is around the corner. There are autonomous trains too, but this technology seems to be developing much slower. Driving a car requires to steer the car to follow the road geometry and to avoid the impact with other vehicles that can move unexpectedly. The train case is clearly easier. The train is not really driven. The wheel-rail geometry makes steering a passive action. Essentially, only the forward velocity is controlled. It seems that autonomous trains are easier to develop than autonomous cars. Autonomous trains would allow the use of smaller train units, with little probability of impact, allowing to increase the density of trains in the track. The development of autonomous trains would be enhanced with better understanding of the train-track dynamics, using low-cost sensors and accurate and adjustable vehicle dynamic models. These technologies will benefit with the development of improved rail multibody models.

Following the comparison with the car transport, safety of the train ride is easier to evaluate or to guarantee by electronic control units (ECU). The scenarios of lack of safety that can occur when driving a car are much more varied than in the case of the train. In the train, safety of the ride is based on criteria (derailment, Prud'homme, wheel unloading and turnover safety criteria) that depend exclusively on the wheel-rail contact forces. However, the development of safety ECU in the railway industry also lags behind that of the automobile industry. The development of dynamic models for the onboard estimation of the wheel-rail contact forces, accounting for the real wheel

profile and rail irregularities, would be of great help to enhance safety ECU's in trains. These technologies can be boosted with the use of onboard rail multibody models.

In addition to good dynamic models, the onboard estimation of wheel-rail forces requires the measurement of wheel geometry (profile shape, equivalent conicity), track geometry (long and short-wave irregularities) and vehicle suspension properties (stiffness and damping coefficients). These values/parameters turn out to be essential in the maintenance of tracks and vehicles. Suspension failures are the most likely cause of a vehicle going to a shop. Wear of the wheel profiles is fundamental for the vehicle dynamics and a key aspect of vehicle maintenance, as it is the track irregularity in track maintenance. Therefore, the ECU that can be used to improve the train ride safety can also be of great help for vehicle and track predictive maintenance. Maintenance in the rail industry is very expensive and the industry needs new methods and techniques to lower it. Treating the mentioned data with Big Data, AI and Cloud Computing techniques will do the rest.

This paper explains the developments in computational and experimental railway dynamics at the University of Seville in the last 20 years. It includes 2 more sections. Section 2 is devoted to advances and simplifications of the computational models of the rail vehicle-track dynamic systems. Section 3 is devoted to industrial applications based on the models developed in Section 2.

2   MULTIBODY MODEL OF THE RAIL VEHICLE-TRACK DYNAMIC SYSTEM

The application of multibody dynamics to railway dynamics has some features that require the development of specific modeling and computational tools. These features are:

1.   The vehicle-track relative motion has more interest that the vehicle absolute motion.
2.   Very long-distance simulations are of interest.
3.   Complex geometry is involved in the definition of the track and the wheel-rail contact interaction.
4.   Modeling the track flexibility is challenging due to its nearly infinite length.

During the last two decades, the research group of the author has developed modeling and simulation tools that account for these features [4-23]. In many cases, these tools involve the simplification and linearization of different terms of the vehicle-track equations of motion. The set of computational tools summarized in this work includes:

1.   Use of non-inertial track frame for the kinematic description of the vehicle-track system.
2.   Modeling of the railway vehicle as a set of open-chain mechanisms.
3.   Use of a non-uniform set of arc-length, track-relative and joint coordinates.
4.   Simplification of generalized inertia forces.
5.   Linearization of generalized suspension forces.
6.   Knife-edge equivalent wheel-rail contact geometry (KEC method).
7.   Moving modes method (MMM) for modeling track flexibility.

This section describes these methods for the simplification of the equations of motion (EOM) of the vehicle-track dynamic system.

2.1 Linear equations of motion

The vehicle-track dynamic system can be considered as a multibody system. As such, the equations of motion (EOM) are a set of differential-algebraic equations (DAE) written in terms of a set of dependent coordinates, and their time-derivatives, and Lagrange multipliers to account for the reaction forces due to the assumed constraint equations. However, the dynamics of the vehicle, and possibly of the track, can be considered as almost linear under certain circumstances. For example, the vertical dynamics of a vehicle modeled with rigid bodies and linear suspension elements travelling on a rigid tangent (straight) track is well modeled using linear ODE. The lateral motion of rail vehicles in tangent or circular tracks [2] can also be modeled with linear ODE. An interesting question is under what conditions, and using what set of generalized coordinates and frames, the multibody DAE can be simplified to linear ODE for railway systems. This question can be expressed as:

$$\begin{cases} \mathbf{M\ddot{q}} + \mathbf{\Phi}_{\mathbf{q}}^T \lambda = \mathbf{Q} + \mathbf{Q}_v \\ \mathbf{\Phi}(\mathbf{q},t) = \mathbf{0} \end{cases} \overset{?}{\Rightarrow} \quad \mathbf{\bar{M}\ddot{q}} + \mathbf{C\dot{q}} + \mathbf{Kq} = \mathbf{F}(t) \tag{1}$$

where $\mathbf{q}$ is the array of generalized coordinates, $\mathbf{M}$ is the coordinate-dependent mass matrix, $\mathbf{\Phi}$ is the array of constraint equations, $\mathbf{Q}$ is the vector of generalized applied forces, $\mathbf{Q}_v$ is the vector of generalized quadratic-velocity inertia terms, $\mathbf{\bar{M}}$ is the value of $\mathbf{M}$ at $\mathbf{q} = \mathbf{0}$, $\mathbf{C}$ is the damping matrix, $\mathbf{K}$ is stiffness matrix and $\mathbf{F}$ is the vector of linearized applied forces.

The author believes that for a track with general geometry no formulation exists that can describe approximately the 3D dynamics of the vehicle-track system using linear ODE. The closest formulation is the *weakly coupled vertical and lateral dynamics formulation* for rail vehicles described in [19]. In this formulation, the generalized coordinates are divided into vertical and lateral coordinates (longitudinal motion is supposed to be prescribed), as follows:

$$\mathbf{q} = \begin{bmatrix} \mathbf{q}_V^T & \mathbf{q}_L^T \end{bmatrix}^T \tag{2}$$

The equations of motion are given by:

$$\begin{aligned} \mathbf{M}_V \mathbf{\ddot{q}}_V^{nw} + \mathbf{C}_V^s \mathbf{\dot{q}}_V + \mathbf{K}_V^s \mathbf{q}_V &= \mathbf{Q}_V \\ \mathbf{M}_L \mathbf{\ddot{q}}_L + \left(\mathbf{C}_L^s + \mathbf{C}_L^c \right) \mathbf{\dot{q}}_L + \left(\mathbf{K}_L^s + \mathbf{K}_L^c \right) \mathbf{q}_L &= \mathbf{Q}_L \end{aligned}, \tag{3}$$

where superscrip s and c stand for *suspension* and *contact*, respectively. Therefore, for the lateral dynamics, there are damping and stiffness matrices associated with the suspension systems and the wheel rail contact. This formulation uses the *equivalent conicity* concept for the wheel-rail contact and linear Kalker theory [2] to calculate the *creep* (contact-tangential) forces. The two set of linear ODE in Eq. (3) cannot be solved independently becuse there are coupling terms. These terms are the reason to call the formulation „weakly coupled" (see [19] for details). The coordinates and frames used in this formulation are described next.

2.2 Generalized coordinates and frames of reference

For the kinematic description of rail vehicles three different frames can be used:

1. The global-inertial frame: $\langle O; X, Y, Z \rangle$
2. The body-track frame (for body *i*): $\langle O^{bti}; X^{bti}, Y^{bti}, Z^{bti} \rangle$
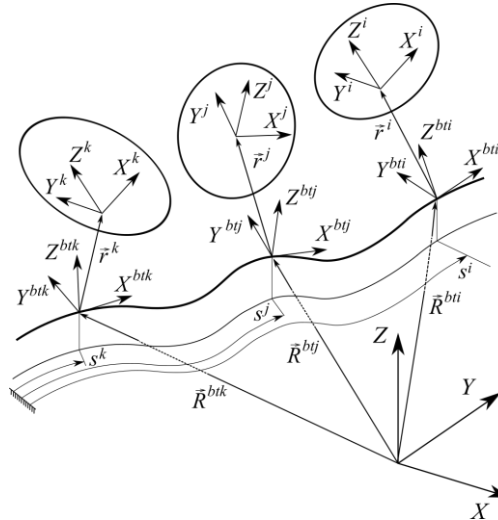3. The body frame: $\langle O^i; X^i, Y^i, Z^i \rangle$

Figure 1. *Kinematics of the bodies of a railway vehicle with relative body-track frame coordinates*

The body-track frame is defined such that the relative position vector $\mathbf{\bar{r}}^i = \begin{bmatrix} 0 & \bar{r}_y^i & \bar{r}_z^i \end{bmatrix}^T$ of the body frame with respect to the body-track frame has zero *x* component along the track centerline. Therefore, for each body *i*, the set of coordinates:

$$\mathbf{q}^i = \begin{bmatrix} s^i & \bar{r}_y^i & \bar{r}_z^i & \left(\bar{\mathbf{\Phi}}^i\right)^T \end{bmatrix} = \begin{bmatrix} s^i & \bar{r}_y^i & \bar{r}_z^i & \bar{\varphi}^i & \bar{\theta}^i & \bar{\psi}^i \end{bmatrix}^T \qquad (4)$$

describes the absolute position of the body-track frame (arc-length coordinate s^i), the relative body frame to body-track frame position (position vector $\bar{\mathbf{r}}^i$) and relative body frame to body-track frame orientation (orientation coordinates $\bar{\mathbf{\Phi}}^i$).

The main advantage of the use of track-relative coordinates instead of absolute reference coordinates is that they facilitate linearization of the equations of motion (EOM) that is very helpful for the steady-state running analysis, stability analysis or curving analysis of the vehicles. On the other hand, the kinematics becomes more involved because the track geometry appears in the calculation of the position and orientation of the bodies.

Other railway formulations use a single track-frame for the kinematic description of the whole railway vehicle [18]. This way, the total number of arc-length coordinates reduces to one. One important advantage of this option, which is not considered in this paper, is that the calculation of the generalized suspension forces is easier because all bodies are descried with respect to the same track-frame. This fact facilitates the calculation of relative distances and their time-derivatives needed to obtain the spring and damping forces. The use of a single-track frame is not so convenient for modeling long trains and/or tracks with narrow curves. In these cases, the relative angles $\bar{\mathbf{\Phi}}^i$ can be so large that kinematic linearization due to small-angles assumption is not recommendable.

2.3 The rail vehicle as a multibody system

Any rail vehicle can be modeled as a set of open-loop chains of bodies connected with spring-dashpot force elements. For each chain i in the vehicle, a *base body* is selected. The generalized coordinates used to describe the motion of the chain includes a set of arc-length and track-relative coordinates $\mathbf{q}_t^i = \begin{bmatrix} s^i & \bar{r}_y^i & \bar{r}_z^i & \bar{\varphi}^i & \bar{\theta}^i & \bar{\psi}^i \end{bmatrix}^T$ (as explained in previous subsection) with respect to the chain-track frame $\left\langle O^{cti}; X^{cti}, Y^{cti}, Z^{cti} \right\rangle$, plus a set of joint-relative coordinates $\mathbf{\Theta}^i$ (usually relative angles) for the kinematic joints, as follows:

$$\mathbf{\Theta}^i = \begin{bmatrix} \mathbf{\Theta}^{i,1T} & \cdots & \mathbf{\Theta}^{i,nkj_i T} \end{bmatrix}^T \qquad (5)$$

Therefore, for each chain, the following set of coordinates can be used:

$$\mathbf{q}^i = \begin{bmatrix} \mathbf{q}_t^i \\ \mathbf{\Theta}^i \end{bmatrix}, \quad i = 1,...,nch \qquad (6)$$

The set of coordinates used for the whole vehicle is given by:

$$\mathbf{q} = \begin{bmatrix} \mathbf{q}^{1T} & \cdots & \mathbf{q}^{nch\,T} \end{bmatrix} \qquad (7)$$

Using this model and set of coordinates, the vehicle-multibody system is constraint-free except for the wheel-rail constraints, in case a constraint-based wheel-rail contact model is used.
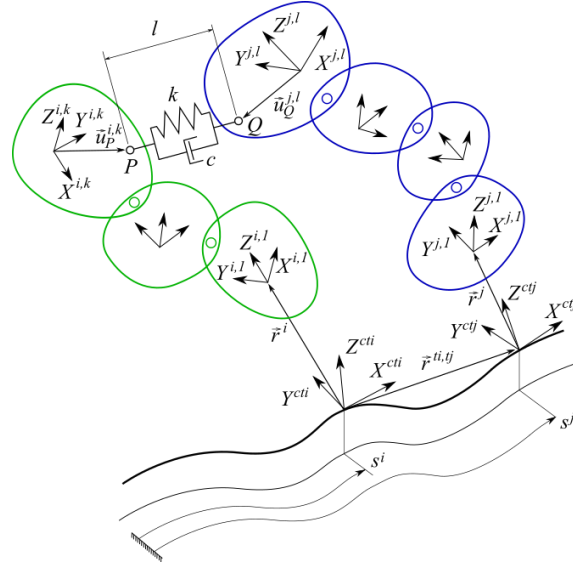
Figure 2. *Model of rail vehicle as a set of open-chain mechanisms.*

2.4 Linearized kinematics

The use of the set of coordinates given in Eqs. (4) – (7) for the description of the vehicle kinematics has the important advantage that all angles can be treated as small angles, with the only exception of the rolling angles of the wheels or wheelsets. The small angle assumption can be used to linearize the rotation matrices considering the sine of the angles equal to the angles and the cosines equal to one. This approximation results in an important simplification of the equations of motion. However, the small angles assumption must be used with care to yield a set of physically meaningful equations.

The use of track-relative coordinates has an important disadvantage that is not that obvious. The kinematic relationship depends on the geometry of the track centerline. That means that the absolute translational velocity $\overline{\mathbf{v}}_G^j$ and angular velocity $\widehat{\boldsymbol{\omega}}^j$ of a rigid body j are functions of the curvatures (horizontal, vertical and twist curvatures) of the track centerline, that in turn are functions of the arc-length coordinate s^j, as follows:

$$
\begin{aligned}
\overline{\mathbf{v}}_G^j &= \mathbf{H}^j \dot{\mathbf{q}}^{ci}, \\
\widehat{\boldsymbol{\omega}}^j &= \mathbf{G}^j \dot{\mathbf{q}}^{ci},
\end{aligned}
\tag{8}
$$

where the *velocity transformation matrices* $\mathbf{H}^j$ and $\mathbf{G}^j$ are functions of the coordinates $\mathbf{q}^{ci}$ and the track geometry. In the case of a single body chain, as any of the bodies shown in Fig. 1, the velocity transformation matrices yield:

$$
\begin{aligned}
\mathbf{H}^i &= \begin{bmatrix}
1 - \rho_h \overline{r}_y^i + \rho_v \overline{r}_z^i & 0 & 0 & 0 & 0 & 0 \\
-\rho_{tw} \overline{r}_z^i & 1 & 0 & 0 & 0 & 0 \\
\rho_{tw} \overline{r}_y^i & 0 & 1 & 0 & 0 & 0
\end{bmatrix}, \\
\mathbf{G}^i &= \begin{bmatrix}
\rho_{tw} - \rho_h \overline{\theta}^i + \rho_v \overline{\psi}^i & 0 & 0 & 1 & 0 & 0 \\
\rho_v + \rho_h \overline{\varphi}^i - \rho_{tw} \overline{\psi}^i & 0 & 0 & 0 & 1 & 0 \\
\rho_h - \rho_v \overline{\varphi}^i + \rho_{tw} \overline{\theta}^i & 0 & 0 & 0 & 0 & 1
\end{bmatrix},
\end{aligned}
\tag{9}
$$

where ρ_h, ρ_v and ρ_{tw} are the horizontal, vertical and twist curvatures of the track centerline, respectively.

A second source of linearization is to neglect the influence of the track geometry in the velocity transformation matrices. Minimum radius of railroad curves in metropolitan trains is about 30 m. Assume that the three curvatures take the (very large) value: $\rho_h = \rho_v = \rho_{tw} = 1/30 = 0.0033\,\mathrm{m}^{-1}$. Assume that the vertical position of the center of gravity of the body with respect to the track is $\bar{r}_z^i = 2$ m (quite high) and the lateral displacement is $\bar{r}_y^i = -0.1$ m (much more that lateral wheel-track clearance), and the relative rotations are 6 degrees ($\bar{\varphi}^i = -\bar{\theta}^i = \bar{\psi}^i = 0.1$ rad , very large relative rotations in railway dynamics). In this case, the velocity transformation matrices yield:

$$\mathbf{H}^i = \begin{bmatrix} 1.07 & 0 & 0 & 0 & 0 & 0 \\ -0.07 & 1 & 0 & 0 & 0 & 0 \\ -0.003 & 0 & 1 & 0 & 0 & 0 \end{bmatrix} \simeq \begin{bmatrix} \mathbf{1}_{3\times3} & \mathbf{0} \end{bmatrix},$$

$$\mathbf{G}^i = \begin{bmatrix} 0.04 & 0 & 0 & 1 & 0 & 0 \\ 0.033 & 0 & 0 & 0 & 1 & 0 \\ 0.027 & 0 & 0 & 0 & 0 & 1 \end{bmatrix} \simeq \begin{bmatrix} \mathbf{0} & \mathbf{1}_{3\times3} \end{bmatrix},$$

(10)

It is now apparent that one can neglect the influence of the track geometry on the velocity transformation matrices $\mathbf{H}^j$ and $\mathbf{G}^j$. The benefits of this simplification will be very large in terms of computational efficiency.

It can be demonstrated that using both, the small angles assumption and neglecting the influence of the track geometry in the velocity transformation matrices, the mass matrix of the chains of bodies i becomes constant.

2.5   Linearized suspension forces

Linearization of the suspension forces, this is, getting the suspension forces simply as $-\mathbf{C}^s\dot{\mathbf{q}} - \mathbf{K}^s\mathbf{q}$, even in the case that the suspension elements show linear constitutive laws, is not a simple task. Consider the example shown in Fig. 3, where the suspension is considered as linear springs acting in the horizonal plane.
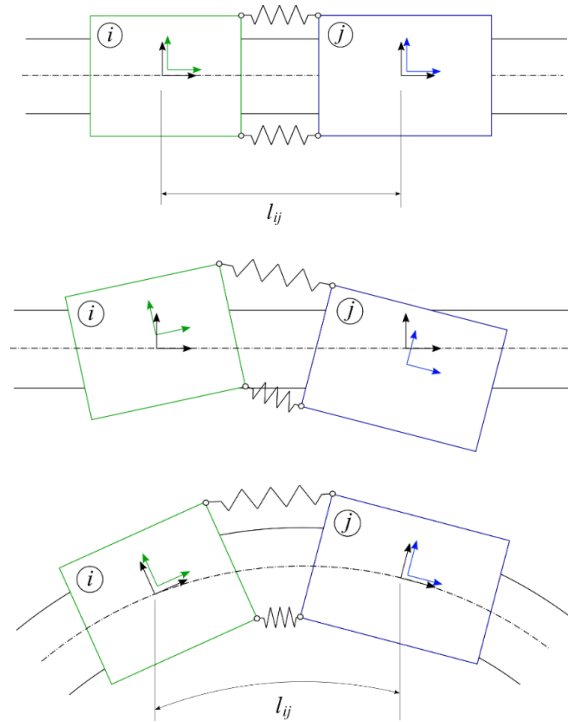

Figure 3. *Bodies connected with suspension elements. Top: reference position in tangent track. Middle:deformed position in tangent track. Bottom: reference position in circular track*

Assume that the linearized spring force is obtained as follows:

$$\mathbf{Q}_{susp}^{lin} = -\mathbf{K}(\mathbf{q} - \mathbf{q}_{ref}), \quad \mathbf{K} = -\left.\frac{\partial \mathbf{Q}_{susp}(\mathbf{q})}{\partial \mathbf{q}}\right|_{\mathbf{q}_{ref}} \tag{11}$$

where $\mathbf{K}$ is the constant stiffness matrix that is obtained as the partial derivative of the nonlinear suspension force $\mathbf{Q}_{susp}$ calculated at a reference value of the coordinates $\mathbf{q}_{ref} = \mathbf{0}$, for which the springs are undeformed. The resulting linearized forces $\mathbf{Q}_{susp}^{lin}$ may provide an accurate value in the deformed position shown in the middle of Fig. 3. However, the linearized forces $\mathbf{Q}_{susp}^{lin}$ are zero in the case shown in the bottom of Fig. 3, where it occurs that $\mathbf{q}_{ref} = \mathbf{0}$, but the spring forces are clearly non zero. This example shows that the simple linearization shown in Eq. (11) does not work. The stiffness matrix clearly depends on the track geometry. A constant geometry-independent stiffness matrix cannot be used for an arbitrary track when using track-relative coordinates.

In the general case in which the suspension elements include spring and dashpots, it can be demonstrated that, for a track with arbitrary geometry, the following approximate linearized expression of the generalized forces:

$$\mathbf{Q}_{susp} \approx \mathbf{Q}_{susp}^{approx-lin} = -\mathbf{K}(\mathbf{q} - \mathbf{q}_{ref}) - \mathbf{C}\dot{\mathbf{q}} - \mathbf{K}^{track}(\mathbf{q}^{ti,tj} - \mathbf{q}_{ref}^{ti,tj}) - \mathbf{C}^{track}\dot{\mathbf{q}}^{ti,tj}, \tag{12}$$

produces accurate results. In this equation $\mathbf{q}^{ti,tj}$ is the set of relative coordinates of track frame tj with respect to track frame ti. and $\mathbf{K}^{track}$ and $\mathbf{C}^{track}$ are constant stiffness and damping matrices associated with the track geometry.

2.5 Knife-edge equivalent contact constraint equations

Wheel-rail contact is the most prominent feature of railway multibody formulation and critical for the dynamic analysis of the vehicle-track. Contact constraint methods use kinematic constraints to reduce the number of degrees of freedom of the wheel-rail system by accounting for the contact conditions.

If the wheel and rail profiles are non-conformal surfaces, the contact constraint for each wheel-rail contact pair is a set of algebraic equations that guarantee that the wheel contact point is located at the same position than the rail contact point and that the tangent plane to the wheel at the contact point is tangent to the tangent plane to the rail at the contact point, as follows:

$$\mathbf{C}_j^C(\mathbf{q}^w, \mathbf{s}) = \begin{vmatrix} \mathbf{R}_C^w(\mathbf{q}^w, \mathbf{s}^w) - \mathbf{R}_C^r(\mathbf{s}^r, s^t) \\ \mathbf{t}_{1C}^{w\ T}\mathbf{n}_C^r \\ \mathbf{t}_{2C}^{w\ T}\mathbf{n}_C^r \end{vmatrix} = \mathbf{0}, \quad j = L, R, \tag{13}$$

where $\mathbf{s}^w$ and $\mathbf{s}^r$ are the two sets of two surface parameters needed to locate the contact point at the surface of the wheel and the rail, respectively, as shown in Fig. 4, $\mathbf{t}_{1C}^w$ and $\mathbf{t}_{2C}^w$ are two tangent vectors to the surface of the wheel at the contact point and $\mathbf{n}_C^r$ is the normal vector to the surface of the rail at the contact point. L and R stand for left and right wheel-rail contact, respectively. Each set of equations of Eq. (13) adds 4 coordinates to the system (4 surface parameters). Therefore, because the number of constraint equations is 5, each contact eliminates 1 degree of freedom of the system. The constraints given in Eq. (13) are among the most complex constraints used in multibody dynamics. The calculation of the Jacobian matrix and its time derivative is very involved. These equations can be simplified assuming that the contact points are in a vertical plane that contains the axle of the wheelset. This approximation, that is very reasonable in most applications, reduces the constraints to:
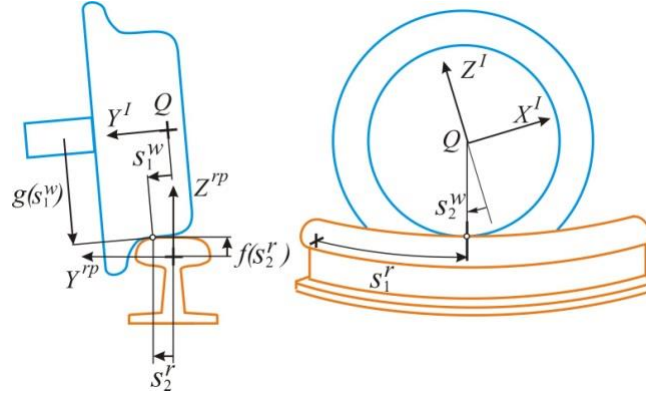
Figure 4. *Wheel-rail contact and surface parameters.*

$$\mathbf{C}_j^C\left(\mathbf{q}^w,\mathbf{s}\right)=\left|\begin{array}{c} \bar{\mathbf{r}}_C^w\left(\mathbf{q}^w,s^w\right)-\bar{\mathbf{r}}_C^r\left(s^r\right) \\ \bar{\mathbf{t}}_C^{wT}\bar{\mathbf{n}}_C^r \end{array}\right|=\mathbf{0},\;\; j=L,R\,, \tag{14}$$

where the position vectors are given in the $<Y^I, Z^I>$ plane (wheelset intermediate frame, a frame that moves with the wheelset but does not show rolling rotation). In Eq. (14) the surface-to-surface contact problem is reduced to a curve-to-curve contact problem. Therefore, the 2 surface parameters for each surface are reduced to 1 curve parameter needed to locate the contact point in the curves. Equation (14) can be solved in a pre-processing stage and the results can be stored in contact lookup tables [18]. This method results in very efficient simulations of railway dynamics.

The KEC-method is based on finding an equivalent profile for the wheel that contacts a rail that is infinitely narrow, such that the subspace of the allowable motion of the wheelset coincides with that of the wheelset and rails with the real profiles. This is shown in Fig. 5.
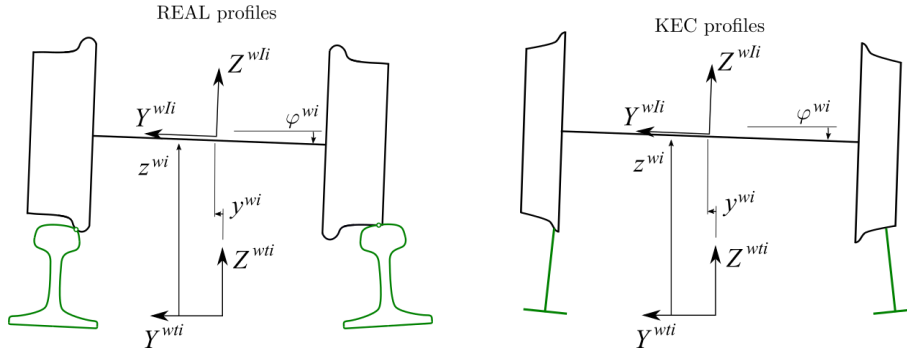

Figure 5. *Wheelset in contact with rails. Left: real wheel and rail profiles.*
Right: equivalent profile on knife-edge rail.

It can be shown [20] that the equivalent profiles exist, and they are very easy to calculate. When using equivalent profiles, constraint equations are almost linear. These equations are:

$$\begin{bmatrix} 0 & r_0+f^{lk} & 1 & 0 \\ 1 & L^w & \varphi^{wi} & 0 \\ 0 & r_0+f^{rk} & 0 & 1 \\ 1 & -L^w & 0 & \varphi^{wi} \end{bmatrix}\begin{bmatrix} \bar{z}^{wi} \\ \varphi^{wi} \\ s^{lk} \\ s^{rk} \end{bmatrix}+\begin{bmatrix} y^{wi}-y^{lir} \\ -f^{lk}-z^{lir} \\ y^{wi}-y^{rir} \\ -f^{rk}-z^{rir} \end{bmatrix}=\mathbf{0}\;\Rightarrow \tag{15}$$

$$\Rightarrow\mathbf{C}^{kec}\left(y^{wi},\mathbf{x}^{wi},\mathbf{x}^{irr}\right)=\mathbf{0}.$$

where $f^{lk}=f^{lk}(s^{lk})$ and $f^{rk}=f^{rk}(s^{rk})$ are the left and right equivalent profiles, that are functions of a curve parameter, y^{lir}, z^{lir}, y^{rir} and z^{rir} are the lateral and vertical, left and right track irregularities.

Table 1 shows the simplification of the constraint equations when using Eq. (13) (exact constraints), Eq. (14) (approximate constraints) and Eq. (15) (KEC). The use of KEC results in railway simulations that are more efficient than the simulations based on lookup tables. Besides, the

use of KEC is the only constraint-based contact approach that can be used to simulate tread and flange contact points simultaneously and wheelset-climbing derailment [21].

Table 1. Simplification of wheel-rail constraint equations.

Constraints	Frame	Number of C	Number of s
Exact	Global	10	8
Approximate	Track	6	4
KEC	Track	4	2

2.6   Moving modes method for modeling track flexibility

The track is a deformable structure with very specific features:

1. It is nearly infinitely long.
2. It can be considered as a space-periodic structure.
3. Deformation is localized in the wheel-rail contact zone.

These features make it very difficult to model the track flexibility using common methods in flexible multibody dynamics for the simulation of small deformations, this is, the *floating frame of reference approach* (FFR). The *moving modes method* (MMM) approach is a computational technique developed by the author's team [7, 13-15,17] with the following properties:

1. Shape functions used for the description of deformation are defined in the track frame. See Fig. 6.
2. It is an *arbitrary Lagrangian-Eulerian* (ALE) method in which the finite element mesh is neither fixed to material points nor fixed to geometric points.
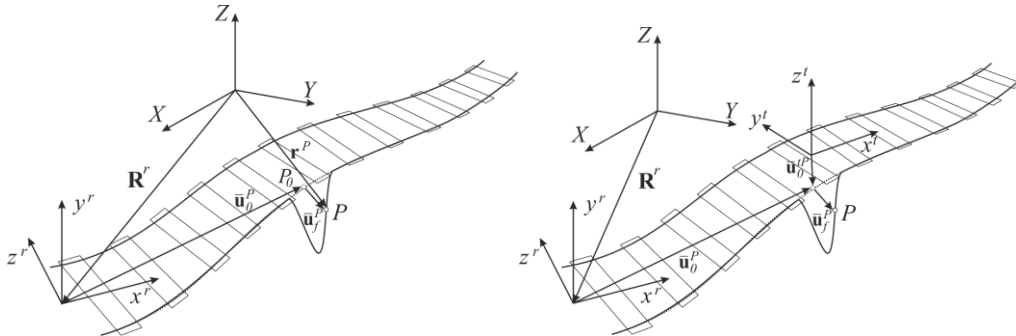

Figure 6. *Modeling track flexibility. Left: floating frame of reference approach. Right: moving modes method approach.*

When using Krylov-subspace model order reduction to find the moving modes [13-14], the Lanczos process guarantee that the *single-input single-output frequency response function* (siso-FRF) of the reduced order model coincides with that of the full order model to the desired degree of accuracy in the desired frequency range. Thus, the MMM allows the accurate simulation of nearly infinite tracks using a few elastic coordinates. Figure 7 shows 5 Krylov-subspace moving modes obtained with the FEM method.
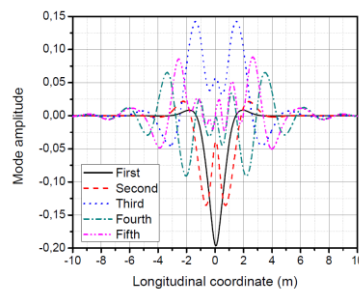

Figure 7. *Krylov-subspace moving modes.*

3 INDUSTRIAL APPLICATIONS

Railway industrial applications at the University of Seville [24-35] have been developed using a 90 m scale track installed at the roof of the School of Engineering and a set of scaled vehicles (see Fig. 8). Some of the developments mentioned in this section have been tested in real scale line vehicles in the Spanish railway system.
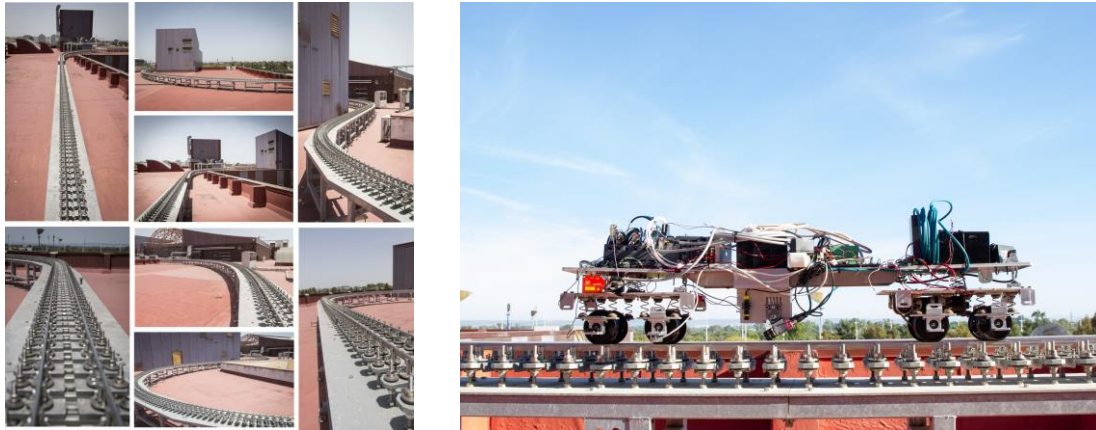

Figure 8. *Experimental facilities. Left: scaled track. Right: scaled rail vehicle.*

All industrial applications described here are intermediate steps in the development of a long-term project: the state observation of the vehicle-track systems, as sketched in Fig. 9. The state observation will be achieved with the help a multibody model of the vehicle-track system that runs on an onboard computer. At least two sensor systems, one to measure the track geometry and another that measures the vehicle dynamic response, will be used to find the inputs for the state observation algorithm. The state observation will be dual: observation of coordinates and velocities and parameter identification. The output of the observation algorithm will be:

1. The dynamics of the vehicle-track system. This output will be very useful for safety and comfort applications.
2. The system parameters. This output will be useful for the *model-base condition monitoring* of the vehicle track system and for the development of intelligent predictive vehicle and track maintenance system.
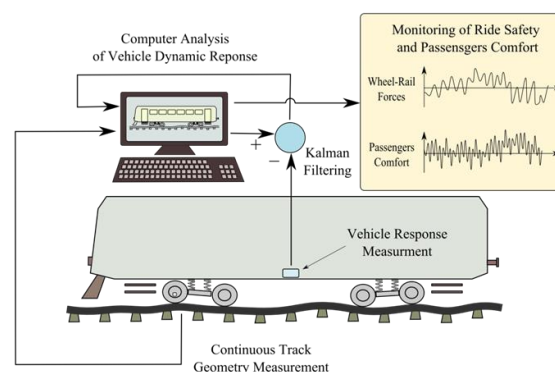

Figure 9. *State observation of the dynamics of the vehicle-track system.*

This is what nowadays is called a *Digital Twin* of the vehicle track system

3.1 Track geometry measuring system

The *track geometry measuring system* (TGMS) [29] is a low cost, accurate mechatronic system that can be installed on line vehicles to measure the track irregularities. It includes inertial sensors and computer vision. The railhead profile is illuminated with a laser projector while a video

camera records the projected line. The system includes a 3D accelerometer and a 3D gyroscope in an *inertial measuring unit* (IMU).
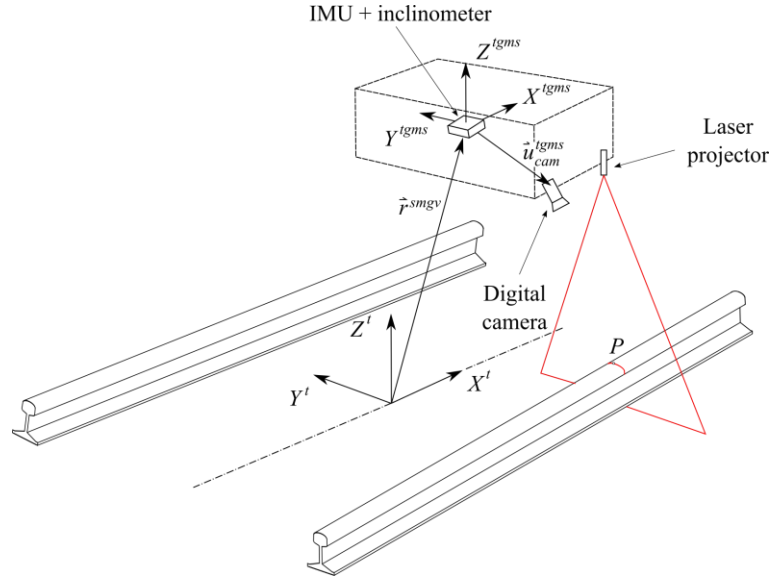

Figure 10. *Track geometry measuring system.*

As described in [29], the profile recorded in the video is a moving curve. Motion of the curve within the frame is due to two factors: (1) that the profile is recorded from a vehicle that has a relative motion with respect to the track, and (2) that the track geometry is irregular. Computer vision and multibody kinematics is used in to develop a numerical algorithm that is able to find the track irregularities and the vehicle dynamics using the recorded video and the measures of the inertial sensors. As shown in Fig. 11, important steps are the calculation of the position and orientation of the railhead frame with respect to the TGMS frame (left of the figure) for each video frame, and the kinematic model that allows the calculation of the track irregularity ($\vec{r}^{lir}$, $\vec{r}^{rir}$) and the vehicle dynamics ($\vec{r}^{tgms}$). This algorithm has been protected in a national patent.
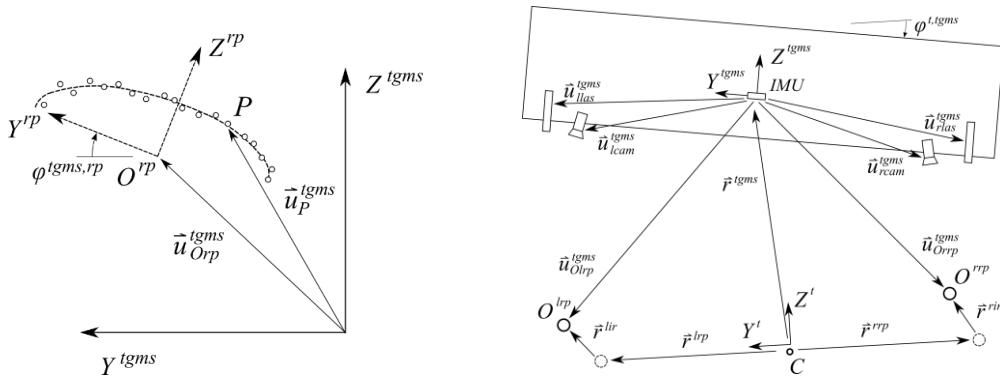

Figure 11. *Track geometry measuring system. Left: calculation of position and orientation of railhead frame. Right: kinematics of the TGMS-irregular track system.*

3.2 Inertial navigation of rail vehicles

Inertial navigation system (INS) is a very well-developed technology for aerial vehicles. The development on INS technology was boosted in the 60's of the last century with the use of Kalman filter in the Apollo project. In fact, INS was the first application for a technique, the Kalman filter, that some authors have described as the most important scientific advance in the XX century. The application of INS to track vehicles is a fundamental step of geometry measurement. The TGMS described in the previous sub-section requires this technology to fine the sensor's absolute position and orientation.

The INS of a rail vehicle is much simpler than that of an aerial vehicle. The reason is that the vehicle follows a trajectory that is very similar to the design geometry of the track centerline. On the other hand, for track geometry measurement, the accuracy requirement of the INS system is millimetric, what is much more than the accuracy needed in aeronautical applications. These facts show that new, specially adapted INS algorithms that are based on the vehicle-track relative kinematics must be developed [36].

The model and measurement equations of an *extended Kalman filter* (EKF) that can be used to find the absolute orientation of the TGMS are given by:

$$\dot{\mathbf{x}} = \begin{bmatrix} \dot{\varphi}^{tgms} \\ \dot{\theta}^{tgms} \end{bmatrix} = \begin{bmatrix} 0 & \hat{\omega}_z^{imu} \\ -\hat{\omega}_z^{imu} & 0 \end{bmatrix} \begin{bmatrix} \varphi^{tgms} \\ \theta^{tgms} \end{bmatrix} + \begin{bmatrix} \hat{\omega}_x^{imu} \\ \hat{\omega}_y^{imu} \end{bmatrix} = \mathbf{F}\mathbf{x} + \mathbf{u}(t)$$

$$\mathbf{z} = \begin{bmatrix} a_x^{imu} \\ a_y^{imu} \end{bmatrix} = \begin{bmatrix} 0 & -g \\ g & 0 \end{bmatrix} \begin{bmatrix} \varphi^{tgms} \\ \theta^{tgms} \end{bmatrix} = \mathbf{H}\mathbf{x}$$

(16)

The model and measurement equations of an EKF that can be used to find the TGMS-track relative position is given by:

$$\dot{\mathbf{x}} = \begin{vmatrix} \dot{r}_y^{tgms} \\ \ddot{r}_y^{tgms} \\ \dddot{r}_y^{tgms} \\ \dot{r}_z^{tgms} \\ \ddot{r}_z^{tgms} \\ \dddot{r}_z^{tgms} \end{vmatrix} = \begin{bmatrix} 0 & 1 & 0 & 0 & 0 & 0 \\ 0 & 0 & 1 & 0 & 0 & 0 \\ 0 & 0 & 0 & 0 & 0 & 0 \\ 0 & 0 & 0 & 0 & 1 & 0 \\ 0 & 0 & 0 & 0 & 0 & 1 \\ 0 & 0 & 0 & 0 & 0 & 0 \end{bmatrix} \begin{vmatrix} r_y^{tgms} \\ \dot{r}_y^{tgms} \\ \ddot{r}_y^{tgms} \\ r_z^{tgms} \\ \dot{r}_z^{tgms} \\ \ddot{r}_z^{tgms} \end{vmatrix} = \mathbf{F}\mathbf{x}$$

(17)

$$\mathbf{z} = \begin{vmatrix} a_y^{imu} + a_x^{imu}\psi^{tgms} - a_z^{imu}\varphi^{tgms} - g\varphi^t - \rho_h V^2 \\ \omega_y^{imu} - \rho_v V \\ 0 \\ a_z^{imu} - a_x^{imu}\theta^{tgms} + a_y^{imu}\varphi^{tgms} - g + \rho_v V^2 \\ \omega_z^{imu} - \rho_h V \\ 0 \end{vmatrix} = \begin{bmatrix} 0 & 0 & 1 & 0 & 0 & 0 \\ 0 & 0 & 0 & 0 & \dfrac{\dot{V}}{V^2} & -\dfrac{1}{V} \\ 1 & 0 & 0 & 0 & 0 & 0 \\ 0 & 0 & 0 & 0 & 0 & 1 \\ 0 & -\dfrac{\dot{V}}{V^2} & \dfrac{1}{V} & 0 & 0 & 0 \\ 0 & 0 & 0 & 1 & 0 & 0 \end{bmatrix} \begin{vmatrix} r_y^{tgms} \\ \dot{r}_y^{tgms} \\ \ddot{r}_y^{tgms} \\ r_z^{tgms} \\ \dot{r}_z^{tgms} \\ \ddot{r}_z^{tgms} \end{vmatrix} = \mathbf{H}\mathbf{x}$$

These are very simple, almost linear Kalman filters, that can be used to find the position and orientation of any rail vehicle body, like the TGMS. The key to the success of these equations is a good estimation of the covariance matrices of the assumed Gaussian-noise of the system model and the measurements model. In [36] a *constrained maximum likelihood estimation* was used with excellent results in geometry measurement.

The INS for rail vehicles is very important in the industry. The trolleys that are used in the industry to measure the track geometry require the use of a *total station* (TS) for the calculation of the trolley trajectory. The TS must be in a fixed position at the side of the track. Therefore, this device must be moved every few tenths of meters, what makes the geometry measurement very slow. The reader can easily understand the important advantage of getting rid of the TS.

3.3 Geometry measurement with only inertial sensors

The use of video cameras in the TGMS can be problematic. Video cameras are more expensive than inertial sensors and they must be used in a very dirty environment. Besides, the computer vision algorithms are complicated and consume a lot of computational time. It would be very convenient to develop a measuring system that uses only inertial sensors [30, 31].
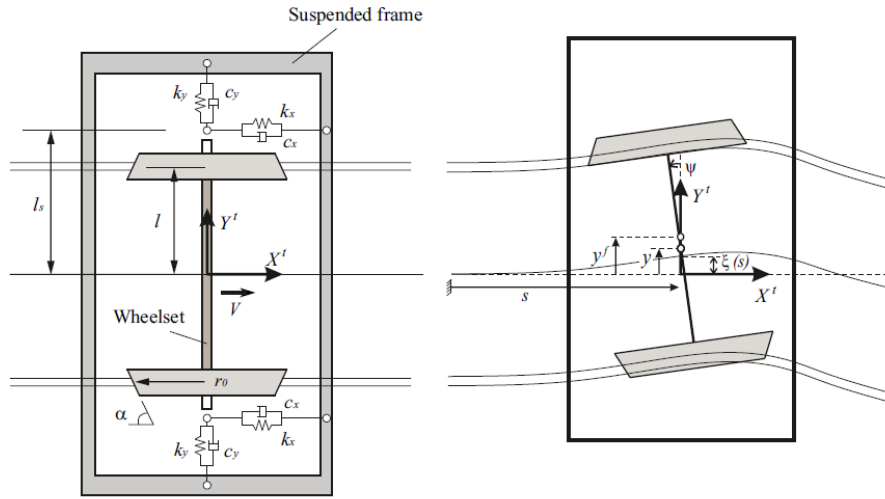
Figure 12. *Plan view of simplified vehicle model.*

The algorithm that finds the track geometry using inertial sensors only is also based on a Kalman filter. However, in this case, the system model, instead of being a simple kinematic model, like in Eqs. (16)-(17), is a dynamic model based on the linear weakly coupled dynamic model described in Sub-section 2.1. The model that is used for the measurement of the alignment uses as model equation the simplified system shown in Fig. 12. The estate vector and measurements vector are given by:

$$\mathbf{x} = \begin{bmatrix} y & \psi & y^f & \dot{y} & \dot{\psi} & \dot{y}^f & \xi \end{bmatrix}^T,$$
$$\mathbf{z} = \begin{bmatrix} \ddot{y}_{meas} & \dot{\psi}_{meas} & \ddot{y}^f_{meas} & \xi_{meas} \end{bmatrix}^T$$

(18)

where the selected coordinates can be observed in Fig. 12 and ξ is the alignment irregularity. The measurement vector $\mathbf{z}$ includes two accelerations and an angular rate given by two accelerometers and one gyroscope, respectively, and a "virtual sensor" of the alignment ξ_{meas} that is always zero. This virtual sensor is successfully used to eliminate the drift in the measured irregularity.

The results of this method are almost as good as the results of the TGMS explained in Sub-section 2.1. However, the main drawback of this method is that it requires the identification of a large set of model parameters. Besides, some parameters are difficult to identify experimentally, like Kalker's linear creep coefficients. The TGMS system model, being kinematic, require only geometric parameters that are easy to identify. In our work, for the dynamic model, the *Temporal Structural Model Updating Method* [30] was successfully used.

3.4 Measurement of wheel-rail contact forces with strain gauges

The measurement of wheel-rail contact forces is very important in the industry. Safety criteria are a based on the values of the vertical and lateral wheel-rail contact forces. Contact forces are the most important factors that affect the wear of the wheel and rail profiles. Therefore, the measurement of the wheel-rail contact forces is also very important for vehicle and track maintenance. Nowadays it is very common that rail administrations ask for dynamometric wheels for the measurement of contact forces.
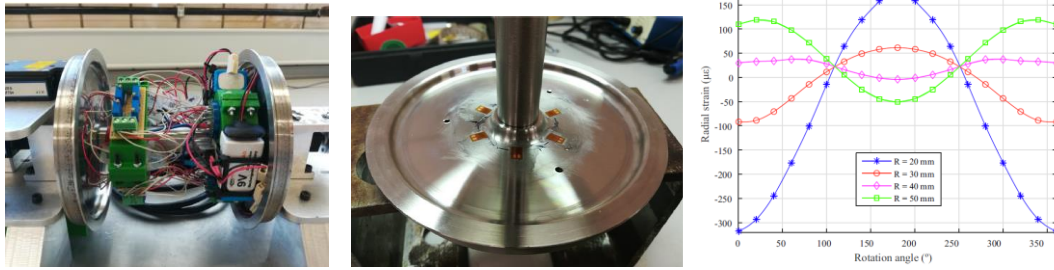
Figure 13. *Extensometric dynamometric wheel.*

The most common method used in the industry to measure the wheel-rail contact forces is the use of wheels instrumented with strain gauges. Strain gauges can be fixed to the wheel web or to the wheelset axle. There are three difficulties with this method:

1. It requires an expensive telemetry system because the gauges are installed in a rotating part.
2. Strains gauges must be very sensitive.
3. The position of the gauges has to be set with high accuracy.

Figure 13 shows on the left shows the scaled dynamometric wheelset with strain gauges. The reader may get an idea of the complicated electronics used. For the calculation of the contact forces, the *harmonic elimination technique* developed by Gutiérrez-López et al [26] was used. However, in [27], an alternative procedure based on artificial neural networks, much more efficieny and equally accurate was developed.

3.5. Measurement of wheel-rail contact forces with distance lasers

An alternative method to measure wheel-rail contact force is based on the use of high precision distance lasers to measure the wheel deformation [26]. The most important benefit of this technique when compared with the extensometry technique is that the sensors are installed in a non-rotating part. Thus, the telemetry system is not needed.
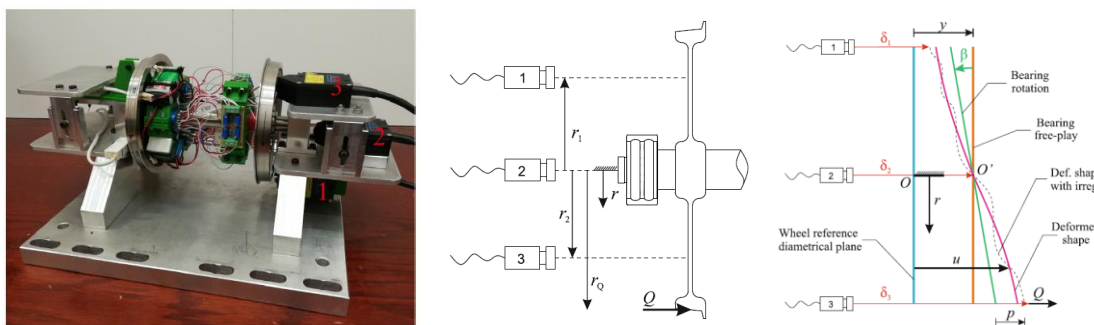

Figure 14. *Dynamometric wheel with distance lasers.*

Figure 14 on the left shows the test bench where both, the extensometry and the distance laser methods, where calibrated. As it can be observed more clearly in the central drawing, three lasers were used. The drawing of the right shows the simple flexible model that was used to find the lateral contact force Q as a function of the three measurements. The results of this research [26] pointed out that the extensometry technique is more accurate than the distance lasers technique, as it can be observed in Fig. 15.
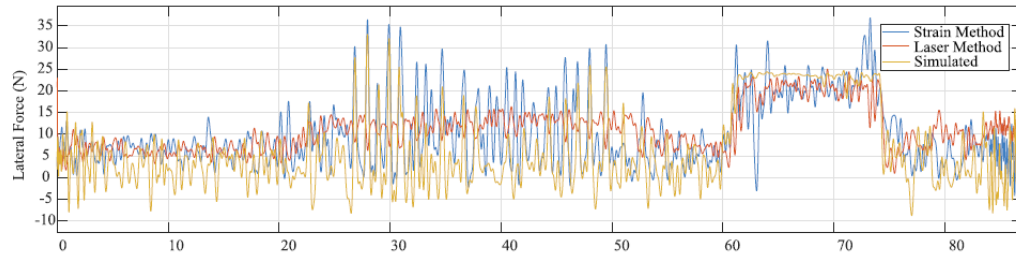
Figure 15. *Comparison of measured and simulated lateral wheel-rail contact forces.*

3.6 Measurement of corrugation

Corrugation is a short wave-length irregularity (between 10 and 1000 mm) that appear in railway tracks. It is very common in curved segement of metropolitan trains and it is a challenging maintenance problem.

Figure 16. *Corrugation in the scale track.*

Our group is developing a method to detect corrugation using *axle-box accelerometers* (ABA). To that end, corrugated track segments have been installed in the scale track, as can be observed in Fig. 16. The corrugation has been machined in the railhead following an analytical profile. That way, a full control of the geometry to be detected is achieved.
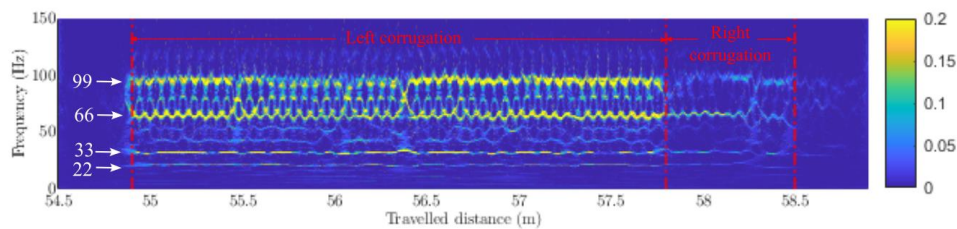

Figure 17. Time-frequency analysis of ABA using *WSST*.

Different signal processing techniques of the measured corrugation-induced acceleration, like *wavelet synchorosqueezed transform* (WSST) shown in Fig. 17, has been successfully used to detect the corrugation wavelengths where they appear. However, the calcuation of a transfer function that can provide an accurate value of the amplitude of the corrugation our of the acceleration signal is still a work in progress.

4. SUMMARY AND CONCLUSIONS

The railroad dynamics research group at the University of Seville has developed a set of development in the modeling and computer simulation of rail vehicles. One of the main objective of these developments is to find simple and accurate models that can describe the vehicle and track dynamics. These developments have been done in the context of multibody dynamics.

However, the purpose of this research is beyond the computer simulation. The models are developed to be run on onboard computers to do the state observation of the vehicle-track system, thus finding the coordinates and velocities of the system (ride quality) and the system parameters (predictive maintenance).

ACKNOWLEDGMENTS

REFERENCES

[1] Garg, V., Dynamics of railway vehicle systems. Elsevier, 2012.

[2] Wickens, A. H., Fundamentals of rail vehicle dynamics. Guidance and stability", Swets & Zeitlinger, 2003.

[3] Esveld, C., Modern Railway Rack, 2nd Ed., MRT-Productions, 2001.

[4] Shabana, A.A., Zaazaa, K.E., Escalona J.L., Sany, J.R., "Development of Elastic Force Model for Wheel/Rail Contact Problems", *Journal of Sound and Vibration*, 269(1-2), 295-325, Elsevier, 2003.

[5] Escalona, J.L., Chamorro, R., "Stability analysis of vehicles on circular motions using multibody dynamics, *Nonlinear Dynamics*, 53, 237-250, 2008.

[6] Rathod, C., Chamorro, R., Escalona, J.L., El-Sibaie, M., Shabana, A.A., "Validation of three-dimensional multibody system approach for modeling track flexibility", *IMechE Journal of Multi-body Dynamics*, 223, 269-282, 2009.

[7] Chamorro, R., Escalona, J.L., González, M.J., "An approach for modelling long flexible bodies with application to railroad dynamics", *Multibody System Dynamics*, 26, 135–152, 2011.

[8] Recuero, A.M., Escalona, J.L., Shabana, A.A., "Finite element analysis of unsupported sleepers using three-dimensional wheel/rail contact formulation", *IMechE Journal of Multi-body Dynamics*. 225(2), 153-165, 2011.

[9] Harper, M.B., Recuero, A.M., Escalona, J.L., Shabana, A.A., "Use of finite element and finite segment methods in modeling rail flexibility: a comparative study", *ASME Journal of Computational and Nonlinear Dynamics*, 7(4), 2012.

[10] Escalona, J.L., Chamorro, R., Recuero, A.M., "Description of methods for eigenvalue analysis of railroad vehicles including track flexibility", *ASME Journal of Computational and Nonlinear Dynamics*, 7(4), 2012.

[11] Recuero, A.M., Escalona, J.L., Chamorro, R., "A trajectory frame-based dynamic formulation for railroad vehicle simulation", *International Journal of Railway Technology*, 1(2), pp. 21-44, 2012.

[12] Escalona, J.L., Sugiyama, H., Shabana, A.A., "Modelling structural flexibility in multibody railroad vehicle systems", *Vehicle System Dynamics*, 51(7), pp.1027-1058, 2013.

[13] Recuero, A.M., Escalona, J.L., "Application of the trajectory coordinate system and the moving modes method approach to railroad dynamics using Krylov subspaces", *Journal of Sound and Vibration*, 332(20), 5177-5191, 2013.

[14] Recuero, A.M., Escalona, J.L., "Dynamics of the coupled railway vehicle-flexible track system with irregularities using a multibody approach with moving modes", *Vehicle System Dynamics*, 52(1), pp. 45-67, 2013.

[15] Chamorro, R., Escalona, J.L., Recuero, A.M., "Stability analysis of multibody systems with long flexible bodies using the moving modes method and its application to railroad dynamics", *ASME Journal of Computational and Nonlinear Dynamics*, 9, 2014.

[16] Recuero, A.M., Aceituno, J.F, Escalona, J.L., Shabana, A.A., "A nonlinear approach for modeling rail flexibility using the absolute nodal coordinate formulation", *Nonlinear Dynamics*, 83, pp. 463-481, 2016.

[17] Recuero, A.M., Escalona, J.L., "Analytical and numerical validation of a moving modes method for traveling interaction on long structures", *ASME Journal of Computational and Nonlinear Dynamics*, 11, 2016.

[18] Escalona, J.L., Aceituno, J.F., "Multibody simulation of railroad vehicles with contact lookup tables", *International Journal of Mechanical Sciences*, 155, 571-582, 2019.

[19] Muñoz, S., Aceituno, J.F., Urda, P., Escalona J.L. "Multibody model of railway vehicles with weakly coupled vertical and lateral dynamics", *Mechanical Systems and Signal Processing*, 115, 570-592, 2019.

[20] Escalona, J.L, Aceituno, J.F, Urda, P, Balling, O., "Railway multibody simulation with the knife-edge-equivalent wheel-rail constraint method", *Multibody System Dynamics*, 48, 373-402, 2020.

[21] Aceituno, J.F., Urda, P, Briales, E., Escalona J.L., "Analysis of the two-point wheel-rail contact scenario using the knife-edge-equivalent contact constraint method", *Mechanism and Machine Theory*, 148,

2020.

[22] Escalona, J.L., Yu, X., Aceituno, J.L., "Wheel-rail contact simulation with lookup tables and KEC profiles: A comparative study", *Multibody System Dynamics*, Accepted for publication, 2020.

[23] Yu, X, Aceituno, J.F, Kurivnen, E, Matikainen, M.K, Korkealaakso, P, Rouinen, A, Jiang, D, Escalona, J.L, Mikkola, A, "Comparison of numerical and computational aspects between two constraint-based contact methods in the description of wheel/rail contacts", *Multibody System Dynamics*, 54, 303-344, 2022.

[24] Aceituno, J.F, Chamorro, R., García-Vallejo, D., Escalona, J.L., "On the design of a scaled railroad vehicle for the validation of computational models", *Mechanism and Machine Theory*, 115, 60-76, 2017.

[25] Aceituno, J.F., Muñoz, S., Chamorro R., Escalona J.L. "An alternative procedure to measure track irregularities. Application to a scaled track", *Measurement*, 137, 417-427, 2019.

[26] Urda, P, Muñoz, S., Aceituno, J.F, Escalona, J.L, "Wheel-rail contact force measurement using strain gauges and distance lasers on a scaled railway vehicle", *Mechanical Systems and Signal Processing*, 138, 2020.

[27] Urda, P, Aceituno, J.F, Muñoz, S., Escalona, J.L, "Artificial neural networks applied to the measurement of lateral wheel-rail contact force: A comparison with a harmonic cancelation method", *Mechanism and Machine Theory*, 153, 2020.

[28] Urda, P, Muñoz, S., Aceituno, J.F, Escalona, J.L, "Application and experimental validation of a multibody model with a weakly coupled lateral and vertical dynamics to a scaled railway vehicle", *Sensors*, 20, 3700, 2020.

[29] Escalona, J.L, Urda, P, Muñoz, S, "A track geometry measuring system based on multibody kinematics, inertial sensors and computer vision", *Sensors*, 21, 683, 2021.

[30] Muñoz, S, Ros, J., Urda, P, Escalona, J., "Estimation of lateral track irregularity through Kalman filtering techniques", *IEEE Access*, 9, 2021.

[31] Muñoz, S, Ros, J. Urda, P, Escalona, J., "Estimation of lateral track irregularity using a Kalman filter. Experimental validation", *Journal of Sound and Vibration*, 504,, 2021.

[32] Urda, P, Aceituno, J.F, Muñoz, S., Escalona, J.L, "Measurement of railroad track irregularities using an automated recording vehicle", *Measurements*, 183, 2021.

[33] Briales, E., Urda, P, Escalona, J.L, "Track frame approach for heading and attitude estimation in operating railways using on-board MEMS sensor and encoder", *Measurements*, 184, 2021.

[34] Muñoz, S, Urda, P, Escalona, J., "Experimental measurement of track irregularities using a scaled track recording vehicle and Kalman filtering techniques", *Mechanical Systems and Signal Processing*, 169, 2022.

[35] Chamorro, R, Aceituno, J.F, Urda, P, del Pozo, E, Escalona, J.L, "Design and manufacture of a scaled railway track with mechanically variable geometry", *Scientific Reports*, 12, 2022.

[36] González-Carbajal, J., Urda, P, Muñoz, S, Escalona, J.L, "Estimation of the trajectory and attitude of railway vehicles using inertial sensors with application to track geometry measurement", Accepted in *Vehicle System Dynamics*, 2023.